Acta Physiologica Sinica, June 25, 2020, 72(3): 263–273
DOI: 10.13294/j.aps.2020.0035 http://www.actaps.com.cn

Original Article

Na^+-K^+-$2Cl^-$ symporter contributes to γ-aminobutyric acid-evoked excitation in rat enteric neurons

LIU Sumei[1, 2, *], ZHENG Lifei[3], NEITZEL Kayla[1], JI Tuo[3], REN Wei[2], QU Mei-Hua[2, 4]

[1]*Department of Biology, College of Science and Health, University of Wisconsin-La Crosse, La Crosse, WI, USA;* [2]*Department of Physiology and Cell Biology, College of Medicine, The Ohio State University, Columbus, OH, USA;* [3]*Department of Physiology and Pathophysiology, School of Basic Medical Science, Capital Medical University, Beijing 100069, China;* [4]*Translational Medical Center, Weifang Second People's Hospital, Weifang 261053, China*

Abstract: Gamma-aminobutyric acid (GABA) is an inhibitory neurotransmitter in the adult central nervous system (CNS), however, it causes excitation in the immature CNS neurons. The shift from GABA-induced depolarization to hyperpolarization in postnatal brain is primarily due to progressive decrease in the expression of the Na^+-K^+-$2Cl^-$ symporter 1 (NKCC1) and increased expression of the K^+-Cl^- cotransporter 2 (KCC2). Unlike CNS neurons, both immature and mature neurons in the enteric nervous system (ENS) are depolarized by GABA. Molecular mechanisms by which GABA excites ENS neurons are unclear. It is understood, however, that the excitatory action depends on elevated intraneuronal Cl^-. We aimed to test a hypothesis that high intracellular Cl^- in ENS neurons is maintained by activity of the NKCCs. We found that NKCC2 immunoreactivity (IR) was expressed in the ENS of the rat colon on postnatal day 1 (P1). The expression level of NKCC2 continuously increased and reached a steady high level on P14 and maintained at that level in adulthood. NKCC1 IR appeared in ENS on P14 and maintained through adulthood. KCC2 IR was not detectable in the ENS in any of the developmental stages. Both NKCC1 IR and NKCC2 IR were co-expressed with $GABA_A$ receptors in ENS neurons. Exogenous GABA (1 mmol/L) caused membrane depolarization in the ENS neurons. The reversal potential of GABA-induced depolarization was about −16 mV. Blockade of NKCC by bumetanide (50 μmol/L) or furosemide (300 μmol/L) suppressed the depolarizing responses to GABA. Bumetanide (50 μmol/L) shifted the reversal potential of GABA-induced depolarization in the hyperpolarizing direction. Neither the KCC blocker DIOA (20 μmol/L) nor the Cl^-/HCO_3^- exchanger inhibitor DIDS (200 μmol/L) suppressed GABA-evoked depolarization. The results suggest that ENS neurons continuously express NKCC2 since P1 and NKCC1 since P14, which contribute to the accumulation of Cl^- in ENS neurons and GABA-evoked depolarization in neonate and adult ENS neurons. These results provide the first direct evidence for the contribution of both NKCC2 and NKCC1 to the $GABA_A$-mediated depolarization.

Key words: Na^+-K^+-$2Cl^-$ symporter; K^+-Cl^- cotransporter; γ-aminobutyric acid; enteric nervous system; intestine

Received 2019-10-21 Accepted 2020-01-29

This work was supported by DK 097460 from the National Institutes of Health, USA, Research Starter Award from the Pharmaceutical Research and Manufacturers of America Foundation, Seed Grant Award from the University of North Carolina Center for Functional GI & Motility Disorders, USA, National Key Research and Development Program, China (No. 2016YFC1302203), and Beijing Natural Science Foundation, China (No. 5172006, ZLF).

Present address for NEITZEL Kayla: Department of Microbiology and Molecular Diagnostics, Wisconsin Diagnostic Laboratories, 9200 W Wisconsin Ave, Milwaukee, WI 53226, USA

Present address for JI Tuo: Department of Neurology, University of Michigan, Ann Arbor, MI 48109, USA

Present address for REN Wei: James L. Winkle College of Pharmacy, University of Cincinnati, 3225 Eden Avenue 136 HPB, Cincinnati, OH 45267, USA

[*]Corresponding author. Tel: +1-608-7856971; Fax: +1-608-7856959; E-mail: sliu@uwlax.edu

钠钾氯共转运体在γ-氨基丁酸引起的肠神经元兴奋中的作用

刘素梅[1, 2, *]，郑丽飞[3]，NEITZEL Kayla[1]，纪 托[3]，REN Wei[2]，曲梅花[2, 4]

[1]美国威斯康星大学拉克罗斯分校科学与健康学院生物学系，威斯康星州拉克罗斯市 54601；[2]美国俄亥俄州立大学医学院生理学与细胞生物学系，俄亥俄州哥伦布市 43210；[3]首都医科大学基础医学院生理学与病理生理学系，北京 100069；[4]潍坊市第二人民医院转化医学中心，潍坊 261053

摘 要：γ-氨基丁酸(γ-aminobutyric acid, GABA)是成年个体中枢神经系统(central nervous system, CNS)的一种抑制性神经递质，但对未成熟CNS神经元有兴奋作用。出生后GABA对CNS神经元的作用由去极化逐渐转为超极化，这种转变主要是由于大脑Na^+-K^+-2Cl^-共运体1 (Na^+-K^+-2Cl^- symporter 1, NKCC1)表达逐渐减少和K^+-Cl^-共运体2 (K^+-Cl^- cotransporter 2, KCC2)表达增加。与CNS神经元不同，肠神经系统(enteric nervous system, ENS)中未成熟和成体神经元都可被GABA去极化。GABA激发ENS神经元兴奋的分子机制尚不清楚，但与ENS神经元内的高Cl^-浓度有关。本研究目的是检验一个假设，即ENS神经元的细胞内高Cl^-浓度是由NKCCs活动维持的。结果显示，NKCC2免疫反应性(immunoreactivity, IR)在出生后第1天(P1)大鼠结肠ENS中出现，随后持续升高，在P14达到稳定的高水平，并在成年后保持在这一水平。NKCC1的IR出现在P14大鼠的ENS中，并维持到成年。在任何发育阶段的大鼠ENS中都检测不到KCC2的IR。在ENS神经元中，NKCC1和NKCC2均与$GABA_A$受体共同表达。外源性GABA (1 mmol/L)可引起ENS神经元膜去极化。GABA诱导的去极化逆转电位约为−16 mV。NKCC抑制剂布美他尼(50 μmol/L)或速尿(300 μmol/L)可显著抑制GABA诱导的去极化。布美他尼(50 μmol/L)使GABA诱导的去极化逆转电位向超极化方向移动。无论是KCC抑制剂DIOA (20 μmol/L)还是Cl^-/HCO_3^-交换抑制剂DIDS (200 μmol/L)对GABA诱发的去极化都没有明显影响。以上结果提示，ENS表达NKCC1和NKCC2，但是不表达KCC2。NKCC1和NKCC2在GABA引起的肠神经元兴奋中起重要作用。

关键词：钠钾氯共转运体；钾氯共转运体；γ-氨基丁酸；肠神经系统；胃肠道
中图分类号：Q48

The Na^+-K^+-2Cl^- symporters (NKCCs) play an important role in the regulation of intracellular Cl^- concentration [1]. Electroneutral in nature, NKCCs do not generate any transmembrane electrical current, but rather contribute to the inwardly directed net Cl^- flux dictated by the Na^+ concentration gradient. Up to date, two NKCC isoforms, NKCC1 and NKCC2, have been identified [1]. NKCC1 is widely expressed in many organs and tissues, including the brain [2]. NKCC2 is primarily expressed in the thick ascending limb of Henle in the kidneys [2], but is also found in the gastrointestinal tract [3–5].

During early postnatal development, expression of NKCC1 in the brain is high, and its activity elevates intraneuronal Cl^- concentration [6]. When Cl^- channels are opened by the action of γ-aminobutyric acid (GABA), a neurotransmitter in the brain, at the $GABA_A$ receptors, the membrane is depolarized due to Cl^- efflux. $GABA_A$-mediated depolarization results in the opening of voltage-gated Ca^{2+} channels and transient increase of $[Ca^{2+}]_i$, which is essential for neuronal differentiation, migration, and synapse maturation [2]. As development proceeds, NKCC1 expression in the brain decreases [6], whereas the expression of a neuronal Cl^- extruding membrane transporter, the K^+-Cl^- cotransporter 2 (KCC2), increases [2, 7]. The transition to KCC2 results in lowering of the intraneuronal Cl^- concentration, which accounts for the characteristic hyperpolarization of the membrane potential by $GABA_A$ activation. The mechanism underlying the progressive shift from $GABA_A$-mediated depolarization to hyperpolarization during postnatal development has been attributed to the gradual decrease in NKCC1 expression and a steady increase in KCC2 expression in the brain [2, 6, 7]. A most recent study shows that KCC2 expression appears at much earlier stage of development (P0–P2) in some brain regions such as the CA3 in the hippocampus [8]. The early appearance of KCC2 is involved in modulation of ongoing giant depolarizing potentials in the hippocampal neuronal networks even during the perinatal period.

GABA is also expressed in the enteric nervous system (ENS), the intrinsic nervous system of the gut. GABA and its synthesizing enzyme, glutamic acid decarboxylase, are found in ENS neurons in guinea pig, rat and human intestine [9–13]. ENS neurons and glia express GABA transporters, which account for the uptake and accumulation of GABA [10, 11, 14]. Unlike neurons in the central nervous system (CNS), both neonatal and

adult ENS neurons are depolarized by $GABA_A$ receptor activation. Intracellular recording with "sharp" microelectrodes in guinea pig ileal myenteric neurons found that both AH- and S-type neurons were depolarized by GABA action at the $GABA_A$ receptors [15–17]. $GABA_A$-mediated depolarization of ENS neurons is a Cl^--dependent, bicuculline-sensitive event, which resembles the depolarizing action of GABA at immature neurons in the brain and other neurons in the adult peripheral nervous system [18–23]. The depolarizing actions of GABA at $GABA_A$ receptors in the ENS neurons may account for GABA-induced acceleration of small and large intestinal peristalsis and increase of intestinal ion secretion [24–28]. Nevertheless, the cellular mechanisms responsible for accumulation of Cl^- in ENS neurons and related GABA-evoked depolarization require clarification.

We reported earlier that adult rat ENS neurons express NKCC2 [4]. A study by Wouters *et al.* found weak expression of NKCC1 in the ENS of adult mice [29]. Less is known about the distribution of KCCs in the gastrointestinal tract. The aims of the present study were to address two questions: (1) whether NKCCs contribute to the membrane depolarization induced by $GABA_A$ receptor activation in ENS neurons; and (2) whether NKCC expression in the ENS demonstrates developmental changes during postnatal maturation.

1 MATERIALS AND METHODS

1.1 *Animals*

Adult male Sprague-Dawley rats (200–300 g; Charles River, Wilmington, MA, USA) were used. The animal care and experimental protocols were approved by the University of Wisconsin-La Crosse and the Ohio State University Laboratory Animal Care and Use Committee and adhered to the U. S. National Institutes of Health Guide for the Care and Use of Laboratory Animals. Adult rats were anaesthetized by intraperitoneal injection of 0.09 mL mixture of ketamine (91 mg/mL) and acepromazine (0.09 mg/mL) per 100 g body weight prior to euthanasia by decapitation. The distal colon was removed and used for immunofluorescent staining, western blotting, or electrophysiological recording according to the methods described in the following paragraphs. To evaluate the expression pattern of NKCC1 and NKCC2 in the developing ENS, Sprague-Dawley rats were bred and housed in the animal facility of the University of Wisconsin-La Crosse. Rats aged postnatal day 1 (P1), P4, P7, P14, and ≥ P28 (adult) were euthanized and the distal colon was removed and used for immunofluorescent staining.

1.2 *Immunofluorescent staining*

Method of immunofluorescent staining of rat colonic longitudinal muscle-myenteric plexus (LMMP) was similar as described in detail elsewhere [4]. Segments of rat distal colon were removed and placed in ice cold Krebs' solution containing (in mmol/L): NaCl, 120.9; KCl, 5.9; $CaCl_2$, 2.5; $MgCl_2$, 1.2; NaH_2PO_4, 1.2; $NaHCO_3$, 14.4; and glucose, 11.5. The colon was opened along the mesenteric border, stretched tautly and pinned out flat onto Sylgard-coated Petri dishes with mucosa side up. Preparations were immediately fixed in Zamboni's fixative (4% formaldehyde plus 1.5% picric acid, prepared in 0.1 mol/L phosphate-buffered saline) for 3 h at room temperature. After fixation, tissues were washed in phosphate-buffered saline (PBS) three times, 10 min each. Whole mounts of the LMMP were dissected from these preparations. The LMMP preparations were incubated in 10% normal donkey serum plus 0.3% Triton X-100 for 30 min at room temperature to minimize non-specific binding and permeabilize the tissues. The preparations were then incubated in primary antibodies for NKCC1 (rabbit, 1:500, Millipore, cat# AB3560P), NKCC2 (rabbit, 1:500, Millipore, cat# AB3562P), or KCC2 (rabbit, 1:200, Millipore, cat# 07-432) overnight at 4 °C. After being washed, the tissues were incubated in indocarbocyanin (Cy3)-labeled donkey anti-rabbit immunoglobulin G (IgG) (Jackson Immuno Research, West Grove, PA, USA) at room temperature for 1 h. The tissues were washed in PBS and cover slipped with VECTASHIELD mounting medium (Vector Labs). Fluorescence labeling was examined under a Nikon Eclipse 90i automated fluorescence microscope. Specificities of the NKCC1, NKCC2, and KCC2 antibodies were characterized previously [4, 8, 30]. Preadsorbing the antibodies with the corresponding blocking peptides also blocked immunostaining.

Double labeling of NKCC1 and NKCC2 with the $GABA_A$ receptor was used to investigate the co-expression of NKCC and $GABA_A$ receptor in ENS neurons. The tissues were first incubated with the primary and secondary antibodies for NKCC1 and NKCC2 as indicated above. Samples were examined under the fluorescence microscope to ensure quality of labeling. The tissues were then washed in PBS and subsequently incubated with the primary antibody against the β_2 subunit of the $GABA_A$ receptor (goat, 1:200, Santa Cruz

Biotechnology, Inc., CA, USA, cat# sc-31427). The tissues were then washed in PBS and incubated with FITC-labeled donkey anti-goat IgG (Jackson ImmunoResearch Laboratories, West Grove, PA, USA) at room temperature for 1 h. After a thorough rinse, the tissues were cover slipped with VECTASHIELD mounting medium and examined under a Nikon Eclipse 90i fluorescence microscope. All images were acquired with a CoolSnap HQ2 monochrome digital camera, stored on disk and analyzed with MetaMorph imaging software (Molecular Devices Corporation, Sunnyvale, CA, USA).

1.3 *Western blots*

Western blot methods were as described in detail in our earlier report on NKCCs[4]. The LMMP preparations from rat distal colon were dissected, washed with PBS, snap frozen in liquid nitrogen immediately after dissection and stored at −80 °C until use. Tissues were homogenized in 300 μL of cold lysis buffer, pH 7.5, containing Nonidet P-40 (0.5%), Tris-HCl (10 mmol/L, pH 8.0), EDTA (1.0 mmol/L), NaCl (150 mmol/L), EGTA (2.0 mmol/L), 0.1% SDS, sodium orthovanadate (1 mmol/L), deoxycholic acid (0.5%), phenylmethanesulfonyl fluoride (1 mmol/L), aprotinin (5 μg/mL), and leupeptin (5 μg/mL), all purchased from Sigma Aldrich. Proteins (200 μg per line) were separated by 8% SDS/PAGE and then transferred to nitrocellulose membranes. The blot was washed with Tris-buffered saline Tween-20 (TBST) and incubated overnight at 4 °C with polyclonal primary antibodies for NKCC1 (1∶500) or NKCC2 (1∶500). Anti-β-actin (1∶5 000, Sigma Aldrich, cat# A5060) antibody was used as a loading control. After washing in TBST, the blot was incubated with IRDye800 conjugated anti-rabbit IgG (1∶5 000, Rockland Immunochemicals Inc., Gilbertsville, PA, USA, cat# 611-132-002) for 1 h at room temperature. The signals were visualized with Odyssey Infrared Imager (LI-COR, Lincoln, NE, USA) and analyzed by ODYSSEY software (version 1.2, LI-COR, Lincoln, NE, USA).

1.4 *Electrophysiology*

The methods used for intracellular recording from enteric neurons in whole-mount preparations of rat colonic LMMP was similar to methods for guinea pig and was described in our earlier report [31]. Transmembrane electrical potentials were recorded with conventional intracellular "sharp" microelectrodes filled with 2% biocytin in 3 mol/L potassium acetate. Electrode resistance ranged between 80 and 180 MΩ. The pre-amplifier (model M-767; World Precision Instruments, Sarasota, FL, USA) was equipped with a bridge circuit for intraneuronal injection of electrical current. Constant current rectangular pulses were delivered by a Grass SD9 stimulator (Grass Instrument Division, Astro-Med Inc., West Warwick, RI, USA). Data were acquired with the PowerLab data acquisition system (AD Instruments, Inc., Colorado Springs, CO, USA) and analyzed with PowerLab Chart v7.1 software. Excitatory postsynaptic potentials (EPSPs) were evoked by focal electrical stimulation of interganglionic fiber tracts with electrodes made of 20-μm diameter Teflon-coated platinum wire and connected through a stimulus-isolation unit (Grass SIN 5) to a Grass S48 stimulator. Neuronal morphology was revealed by passing hyperpolarizing current (0.5 nA for 10–30 min) to inject biocytin into the neuron from the microelectrode and later histochemical development of the intraneuronal biocytin according to the procedures used in our earlier reports [31]. At the end of each recording session, the preparations were transferred to a chamber filled with Zamboni's fixative and stored at 4 °C overnight. The preparations were cleared in dimethyl sulfoxide (DMSO), rinsed with PBS, and then reacted with fluorescein isothiocyanate (FITC) streptavidin (Vector Labs, Burlingame, CA, USA), diluted 1∶200, for 30 min at 37 °C. The preparations were examined with a Nikon Eclipse 90i automated fluorescent microscope (Nikon Instruments, Inc., Melville, NY, USA) for quality of staining and further processed for immunofluorescence staining for NKCC1 and NKCC2 according to the methods described in the previous paragraph.

1.5 *Chemicals*

Pharmacological agents were applied either by addition to the bathing solution or by pressure micro-ejection with N_2 pulses of controlled duration and pressure from glass micropipettes that had tip diameters of 10–15 μm. GABA was in pulses ranging from 20 ms to 2 s in duration. The pharmacological agents used in this study and their sources were as follows: GABA, bicuculline, biocytin, bumetanide, furosemide, dihydroindenyloxyalkanoic acid (DIOA), and 4,4'-diisothiocyanatostilbene-2,2'-disulfonic acid disodium salt hydrate (DIDS), all from Sigma Aldrich (St. Louis, MO, USA). Stock solutions of bumetanide, furosemide, DIOA, and DIDS were prepared in DMSO. Final concentrations of DMSO were less than 0.1% (v/v). Preliminary experiments indicated that the vehicle did not alter any base-

line electrophysiological activities of enteric neurons. Stock solutions were prepared in Krebs solution and stored at −20°C. Serial dilutions were prepared fresh daily in Krebs solution.

1.6 *Data analysis*

Data are expressed as means ± SEM with *n* values representing the numbers of neurons for electrophysiological studies. Paired or unpaired Student's *t*-test was used to determine statistical significance. $P < 0.05$ was considered statistically significant.

2 RESULTS

2.1 Developmental expression of NKCC1 and NKCC2 in ENS

Immunofluorescent staining of dissected LMMP from

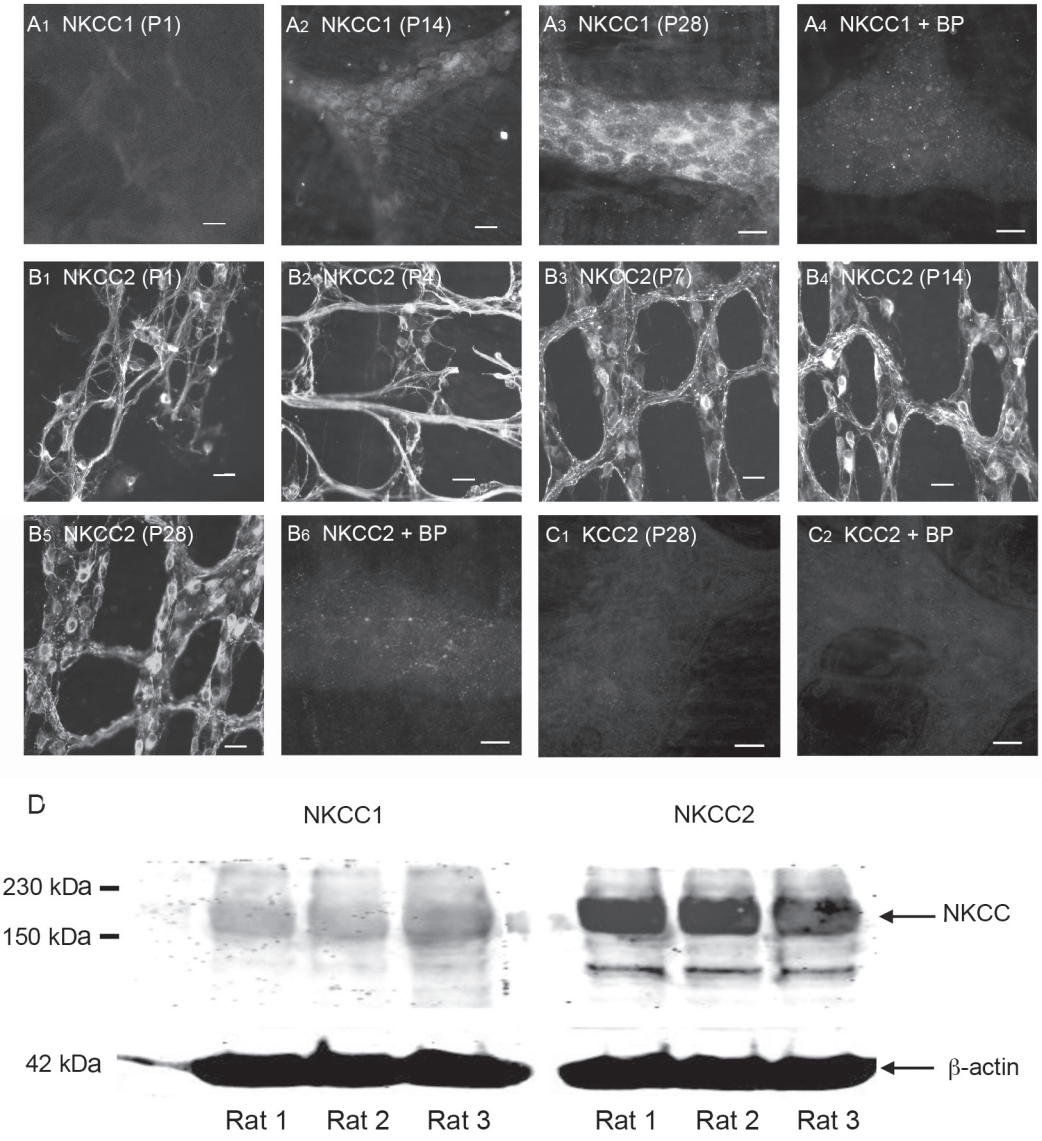

Fig. 1. Developmental expression of Na^+-K^+-$2Cl^-$ symporter 1 (NKCC1), NKCC2, and K^+-Cl^- cotransporter 2 (KCC2) in the rat enteric nervous system (ENS). Immunofluorescent staining of dissected longitudinal muscle-myenteric plexus (LMMP) from the rat colon showed a pronounced developmental up-regulation of NKCCs in the ENS. NKCC1 immunoreactivity (IR) was barely detectable on postnatal day 1 (P1) (A_1). An increase in NKCC1 IR was evident on P14 (A_2) and stabilized on P28 (A_3). NKCC2 IR was evident on P1 (B_1), continuously increased through P4–P7 (B_{2-3}), and stabilized at a high level after P14 (B_{4-5}). In contrast to NKCC1 and NKCC2, IR for the neuronal isoform of chloride extruder, KCC2, was not found in the LMMP (C_1). Pre-adsorption of the antibodies with their corresponding blocking peptides (BP) resulted in no immunostaining (A_4, B_6, C_2). Western blots confirmed the expression of NKCC1 and NKCC2 protein in LMMP preparations from the rat colon (*D*). Scale bars, 20 μm.

the rat colon showed a pronounced developmental up-regulation of NKCC1 expression. NKCC1 immunoreactivity (IR) was barely detectable on P1 (Fig. 1A_1) and P7 (data not shown). An increase in NKCC1 IR was evident on P14 (Fig. 1A_2), and stabilized in adult (P28, Fig. 1A_3). In contrast, expression of NKCC2 IR was evident on P1 (Fig. 1B_1), continuously increased through P4–P7 (Fig. 1$B_{2–3}$), and stabilized at a high level after P14 (Fig. 1$B_{4–5}$). In contrast to NKCC1 and NKCC2, IR for the neuronal isoform of chloride extruder, KCC2, was not found in the LMMP in any of the postnatal developmental stages (Fig. 1C_1).

In adult ENS neurons, NKCC1 and NKCC2 IRs were localized at the surfaces of the neuronal cell bodies, cytoplasm, and proximal segments of the neuronal processes (Fig. 1A_3, B_5). Western blots of membrane proteins, isolated from the dissected LMMP of the adult rat colon, showed that both NKCC1 (~160 kDa) and NKCC2 (~160 kDa) were expressed (Fig. 1*D*).

2.2 Colocalization of NKCC and $GABA_A$ receptors in ENS neurons

We used double-labeling immunofluorescent staining to investigate the colocalized expression of the $GABA_A$ receptors and NKCC in the rat myenteric neurons. NKCC1 and NKCC2 IRs were found to be expressed on the same neurons showing $GABA_A$ receptor IR (Fig. 2).

2.3 Inhibition of GABA-evoked depolarization in ENS neurons by NKCC blockers

Intracellular "sharp" microelectrode recordings were made to study the effects of NKCC blockers on GABA-evoked membrane depolarization in ENS neurons. Data were obtained from 39 neurons in the myenteric plexus of rat distal colon. These neurons had a mean resting membrane potential of (−57.4 ± 2.0) mV (n = 39) and a mean input resistance of (145.2 ± 8.8) MΩ (n = 39). About 51% (20/39) of the neurons fired one or two potentials at the onset of rectangular depolarizing current pulses. Each of these neurons received fast EPSP input in response to focal electrical stimulation applied to interganglionic fiber tracts and therefore satisfied criteria for classification as S-type ENS neurons in the rat [32, 33]. In 39% of neurons (15/39), a single impulse was followed by a characteristic prolonged membrane after-hyperpolarization (AH). These neurons were classified as AH-type ENS neurons [34]. A small subset of neurons (4/39, 10%) received electrically-evoked fast nicotinic EPSP input. However, action potentials could not be evoked in these neurons by intraneuronal injection of super maximal depolarizing current pulses. These neurons fit the description for type 3 neurons reported by Browning and Lee [33].

Application of 1 mmol/L GABA by pressure microejection induced a rapidly-activating membrane depolarization in rat colonic myenteric neurons that was similar to that observed in myenteric neurons of guinea pig ileum [15, 16] and rat duodenum [32]. GABA-evoked depolarization was found in each of the 15 AH-type and 11 of the 20 S-type myenteric neurons, but in none of the type 3 neurons. GABA-evoked depolarization was associated with decreased input resistance in both

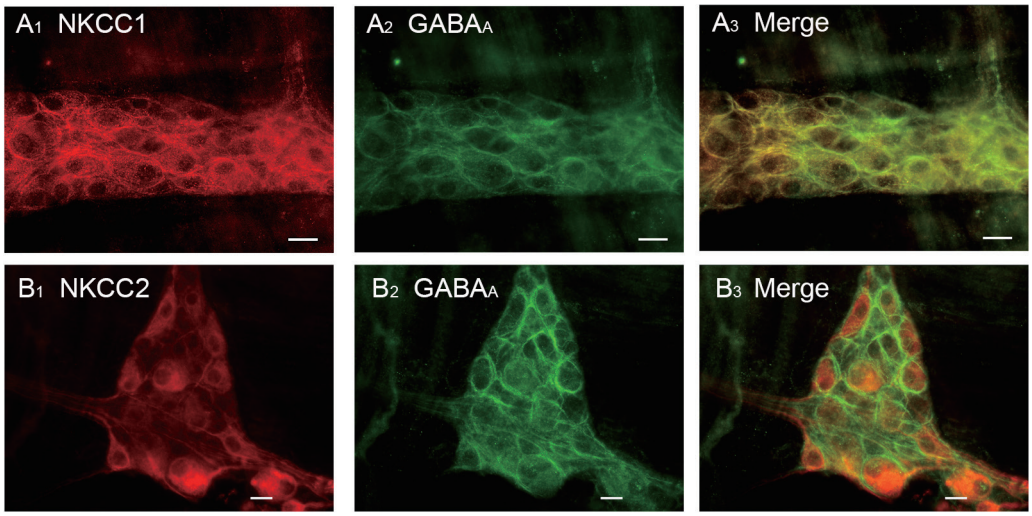

Fig. 2. Immunoreactivity (IR) for NKCC1 and NKCC2 was co-expressed with $GABA_A$ receptor in LMMP of the rat colon. $A_{1–3}$: Co-expression of NKCC1 IR with $GABA_A$ receptor IR. $B_{1–3}$: Colocalization of NKCC2 IR with $GABA_A$ receptor IR. Scale bars, 20 μm.

AH- and S-type neurons (data not shown). Bicuculline (10 μmol/L), which is a $GABA_A$ receptor antagonist, reversibly suppressed the depolarizing responses evoked by GABA (control 12.0 mV ± 1.8 mV *vs* 2.5 mV ± 0.2 mV in bicuculline; $P < 0.01$; $n = 6$).

The loop diuretic bumetanide blocks both NKCC1 and NKCC2 and thereby lowers intracellular Cl^- concentration [35]. We used bumetanide as a pharmacological tool to test the hypothesis that activity of NKCCs accounts for the elevated intraneuronal Cl^- concentrations necessary for GABA-evoked membrane depolarization in ENS neurons. The concentration of bumetanide was chosen based on our previous published studies which showed that 10–100 μmol/L were high enough to block NKCC1 and NKCC2 activities in rat intestinal epithelium [5, 36, 37]. When GABA (1 mmol/L) was applied by micro-pressure ejection (50 ms) in the presence of 50 μmol/L bumetanide in the bathing medium, the amplitude of responses to GABA was reduced by (62.7 ± 2.9)% (control 10.0 mV ± 1.3 mV *vs* 3.7 mV ± 0.4 mV in bumetanide; $P < 0.001$; $n = 9$) (Fig. 3). Another loop diuretic furosemide, which blocks both NKCC and KCC, is less potent than bumetanide in inhibition of NKCC1 and NKCC2 activities [35]. Furosemide (2 mmol/L) has previously been shown to block glycine-induced depolarization in enteric neurons by lowering intracellular Cl^- concentration [38]. Following bath superfusion of furosemide (300 μmol/L), GABA-evoked depolarization was reduced by (45.0 ± 7.6)% (control 12.6 mV ± 1.8 mV *vs* 7.2 mV ± 1.6 mV in furosemide; $P < 0.001$; $n = 5$) (Fig. 3). The KCC blocker, DIOA (20 μmol/L), had no effect on GABA-evoked depolarizing responses (control 12.2 mV ± 2.0 mV *vs* 12.4 mV ± 1.9 mV in DIOA; $P > 0.05$; $n = 5$) (Fig. 3); this concentration of DIOA has been demonstrated to inhibit KCC2 in rat hippocampal neurons [39]. Likewise, inhibition of Cl^--HCO_3^- exchange by DIDS (200 μmol/L) did not suppress GABA-evoked depolarizing responses (control 12.2 mV ± 1.6 mV *vs* 13.0 mV ± 2.0 mV in DIDS; $P > 0.05$; $n = 5$) (Fig. 3), although this concentration of DIDS has been shown to inhibit Cl^--HCO_3^- exchanger activity in rat intestinal epithelium [37]. None of bumetanide, furosemide, DIOA and DIDS altered the resting membrane potential or input resistance of enteric neurons (data not shown).

2.4 Reversal potential of GABA-evoked depolarization in ENS neurons

We determined the reversal potential of GABA-evoked depolarization in the presence and absence of 50 μmol/L bumetanide. GABA (1 mmol/L) was applied, while the

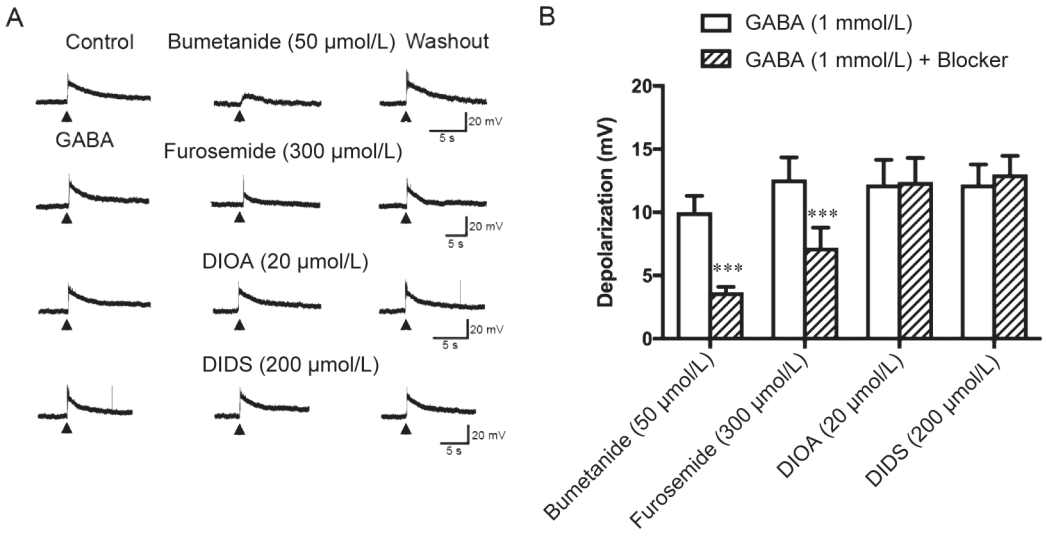

Fig. 3. Pharmacological analysis of membrane depolarizing responses to GABA in myenteric neurons of the rat colon, including effects of the NKCC symporter blockers bumetanide and furosemide, the KCC blocker DIOA, and the Cl^-/HCO_3^- exchanger inhibitor DIDS. *A*: Amplitude of the depolarizing responses evoked by micro-pressure application of GABA (1 mmol/L, 50 ms) was reduced after blockade of the NKCCs with bumetanide or furosamide. Neither the KCC blocker DIOA, nor inhibition of the Cl^-/HCO_3^- exchanger by DIDS, suppressed the GABA-evoked membrane depolarizing responses. *B*: Quantitative data for the effect of the Cl^- transporter blockers on GABA-evoked membrane depolarization. Paired Student's *t*-test was used to determine statistical significance. Means ± SEM. $^{***}P < 0.001$ *vs* GABA.

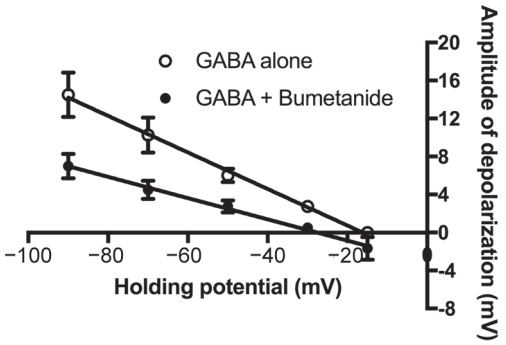

Fig. 4. The NKCC blocker, bumetanide, caused the reversal potential for GABA-evoked depolarizing responses to shift in the hyperpolarizing direction. GABA (1 mmol/L, 50 ms) was applied by pressure micro-ejection, while the membrane potential was current clamped at different levels. The amplitude of the depolarization was plotted against the holding potential and a linear fit was extrapolated to the reversal potential. The reversal potential for GABA-evoked depolarization was near a membrane potential of −16 mV. In the presence of bumetanide (50 μmol/L), GABA-evoked depolarization reversed at a more hyperpolarizing potential (~−28 mV). Means ± SEM.

membrane potential was current-clamped at −90, −70, −50, −30, and −15 mV. The amplitudes of the GABA-evoked depolarization were plotted against the holding potential and the reversal potential was extrapolated from linear fit. The GABA-evoked depolarization reversed at membrane potentials of (−16.18 ± 2.02) mV (n = 4). In the presence of bumetanide (50 μmol/L), the reversal potentials for GABA-evoked depolarization shifted to more negative potentials (−27.63 mV ± 2.41 mV; n = 4; P < 0.001, Fig. 4). Using the Nernst equation, we approximated the intraneuronal Cl^- concentration to be (67.42 ± 6.57) mmol/L (n = 4) in the absence of bumetanide, which was reduced to (44.49 ± 10.28) mmol/L (n = 4) in the presence of 50 μmol/L bumetanide (P < 0.01). This suggested an ongoing Cl^- influx in rat ENS neurons mediated by the bumetanide-sensitive NKCC symporters.

2.5 Expression of NKCC on GABA-responsive ENS neurons

We determined, by filling the neurons with biocytin and subsequent immunostaining the same neurons for either NKCC1 or NKCC2, whether all the neurons that responded to GABA expressed NKCC1 or NKCC2. Five GABA-responsive neurons were stained with the NKCC1 antibody, and all of the neurons expressed NKCC1 (Fig. 5$A_{1–3}$). Four different GABA-responsive neurons were tested for NKCC2 expression and all of them showed NKCC2 IR (Fig. 5$B_{1–3}$).

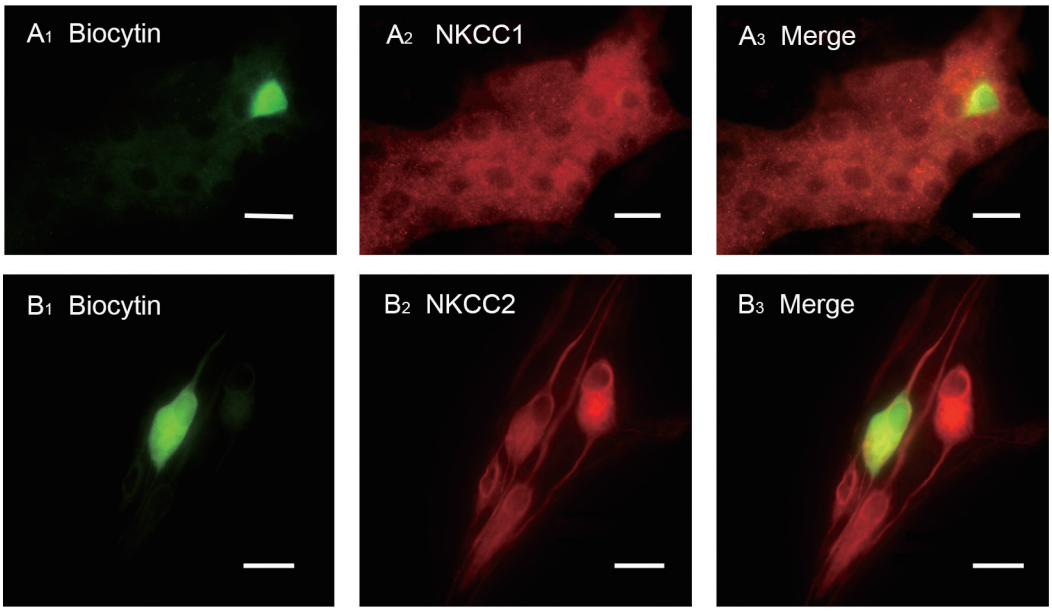

Fig. 5. Expression of NKCC1 and NKCC2 by neurons in which GABA evoked depolarizing responses in the longitudinal muscle-myenteric plexus (LMMP) of the rat colon. $A_{1–3}$: A biocytin-filled neuron, in which GABA evoked depolarizing responses, showed IR for NKCC1. $B_{1–3}$: A biocytin-filled neuron, in which GABA evoked depolarizing responses, expressed discernible IR for NKCC2. Scale bars, 20 μm.

3 DISCUSSION

$GABA_A$-mediated neuronal responses appear as either hyperpolarization or depolarization, depending on the intracellular Cl^- concentration. Immature neurons in the brain sequester cytoplasmic Cl^- at relatively high concentration. In these cases, opening of Cl^- channels leads to Cl^- efflux and depolarization of the membrane potential [40]. NKCC1 is present at high level in early developing brain and appears to be the main transporter responsible for the accumulation of intraneuronal Cl^- and $GABA_A$-mediated depolarization in neonatal neurons [6]. During postnatal brain development, NKCC1 level wanes down, whereas KCC2 expression gradually increases and reaches a steady level by the end of the second postnatal week [2, 6, 7]. The developmental shift from NKCC1 to KCC2 expression in the brain results in lower intraneuronal Cl^- concentration and the characteristic $GABA_A$-mediated hyperpolarization.

We found in the present study that in contrast to CNS neurons, the ENS neurons do not demonstrate the developmental shift from NKCC1 to KCC2. Instead, NKCC1 level is scarce in neonate ENS and appeared in ENS on P14. KCC2 cannot be detected in the ENS at any developmental stage. On the other hand, NKCC2 level is evident in neonate ENS, continuously increases through postnatal development, and stabilizes after P14. Functionally, GABA evokes membrane depolarization in both neonatal and adult ENS neurons [15–17]. Like the immature CNS neurons, ENS neurons have elevated intracellular Cl^- concentration [38, 41, 42]. Our findings support the hypothesis that transport activity of the NKCC1 and NKCC2 accounts for elevation of intraneuronal Cl^- and GABA-evoked depolarizing responses in ENS neurons. During the first two weeks of postnatal development, NKCC2 might be the primary membrane transporter to accumulate intraneuronal Cl^- in ENS. As the ENS development continues, NKCC1 appears and starts to contribute to intraneuronal Cl^- accumulation.

We reported earlier that NKCC2 is expressed by ENS neurons throughout the rat gastrointestinal tract [4]. Wouters *et al*. found faint expression of NKCC1 IR in myenteric ganglia of mouse and human intestine [29]. In the presence study, we confirmed that NKCC1 or NKCC2 IR was present on the same ENS neurons showing $GAGA_A$ receptor IR and GABA-induced depolarization. These results provide strong anatomical evidence that NKCC1 and NKCC2 are involved in $GABA_A$-mediated depolarization in ENS neurons.

The loop diuretics bumetanide and furosemide are established blockers of the NKCCs [35]. To inhibit the activities of NKCC1 and NKCC2, we superfused bumetanide and furosemide in the bathing solution for the LMMP during intracellular recording. Both bumetanide and furosemide decreased GABA-induced depolarization in myenteric neurons. In addition, bumetanide shifted the reversal potential for the GABA-evoked depolarization to a more negative potential. The results strongly suggest that maintenance of high intraneuronal Cl^- is due to the activities of NKCCs, which is necessary for the depolarizing action of GABA in ENS neurons. Unfortunately, the relative contribution of NKCC1 and NKCC2 cannot be deduced from the present results because bumetanide and furosemide inhibit rat NKCC1 and NKCC2 with similar potency [35]. Activities of other Cl^- transporters, such as KCCs or Cl^-/HCO_3^- exchanger, might be involved in the maintenance of intraneuronal Cl^- homeostasis, thus influence $GABA_A$-mediated neuronal actions [2, 7, 43]. However, the roles of KCC2 or Cl^-/HCO_3^- exchanger can be ruled out because neither the Cl^-/HCO_3^- exchanger blocker DIDS, nor the KCC2 blocker DIOA, inhibited GABA-induced membrane depolarization in ENS neurons.

In summary, our results show that myenteric neurons express NKCC1 and NKCC2, which contribute to the accumulation of Cl^- in ENS neurons and GABA/glycine-evoked depolarizing responses in these neurons. To our knowledge, these results provide the first direct evidence for the contribution of both NKCC2 and NKCC1 to the $GABA_A$-mediated depolarization. Since GABA and glycine act as excitatory neurotransmitters in the ENS, understanding the molecular mechanisms of the excitatory actions of these neurotransmitters may provide new insights in the regulation of gut functions controlled by these neurotransmitters, such as smooth muscle activity and epithelial ion transport.

REFERENCES

1 Delpire E, Gagnon KB. Na^+-K^+-$2Cl^-$ cotransporter (NKCC) physiological function in nonpolarized cells and transporting epithelia. Compr Physiol 2018; 8(2): 871–901.

2 Payne JA, Rivera C, Voipio J, Kaila K. Cation-chloride co-transporters in neuronal communication, development and trauma. Trends Neurosci 2003; 26(4): 199–206.

3 Ji T, Liu S, Zheng LF, Wang Q, Dou ZF, Zhang Y, Zhu JX. Cellular distribution of NKCC2 in the gastric mucosa and its

response to short-term osmotic shock. Cell Tissue Res 2012; 348(1): 155–165.

4 Xue H, Liu S, Ji T, Ren W, Zhang XH, Zheng LF, Wood JD, Zhu JX. Expression of NKCC2 in the rat gastrointestinal tract. Neurogastroenterol Motil 2009; 21(10): 1068-e89.

5 Zhu JX, Xue H, Ji T, Xing Y. Cellular localization of NKCC2 and its possible role in the Cl^- absorption in the rat and human distal colonic epithelia. Transl Res 2011; 158(3): 146–154.

6 Plotkin MD, Snyder EY, Hebert SC, Delpire E. Expression of the Na-K-2Cl cotransporter is developmentally regulated in postnatal rat brains: a possible mechanism underlying GABA's excitatory role in immature brain. J Neurobiol 1997; 33(6): 781–795.

7 Rivera C, Voipio J, Payne JA, Ruusuvuori E, Lahtinen H, Lamsa K, Pirvola U, Saarma M, Kaila K. The K^+/Cl^- co-transporter KCC2 renders GABA hyperpolarizing during neuronal maturation. Nature 1999; 397(6716): 251–255.

8 Spoljaric I, Spoljaric A, Mavrovic M, Seja P, Puskarjov M, Kaila K. KCC2-mediated Cl^- extrusion modulates spontaneous hippocampal network events in perinatal rats and mice. Cell Rep 2019; 26(5): 1073–1081.e3.

9 Jessen KR, Hills JM, Saffrey MJ. Immunohistochemical demonstration of GABAergic neurons in the enteric nervous system. J Neurosci 1986; 6(6): 1628–1634.

10 Jessen KR, Mirsky R, Dennison ME, Burnstock G. GABA may be a neurotransmitter in the vertebrate peripheral nervous system. Nature 1979; 281(5726): 71–74.

11 Furness JB, Trussell DC, Pompolo S, Bornstein JC, Maley BE, Storm-Mathisen J. Shapes and projections of neurons with immunoreactivity for gamma-aminobutyric acid in the guinea-pig small intestine. Cell Tissue Res 1989; 256(2): 293–301.

12 Williamson S, Pompolo S, Furness JB. GABA and nitric oxide synthase immunoreactivities are colocalized in a subset of inhibitory motor neurons of the guinea-pig small intestine. Cell Tissue Res 1996; 284(1): 29–37.

13 Nichols K, Staines W, Wu JY, Krantis A. Immunopositive GABAergic neural sites display nitric oxide synthase-related NADPH diaphorase activity in the human colon. J Auton Nerv Syst 1995; 50(3): 253–262.

14 Fletcher EL, Clark MJ, Furness JB. Neuronal and glial localization of GABA transporter immunoreactivity in the myenteric plexus. Cell Tissue Res 2002; 308(3): 339–346.

15 Cherubini E, North RA. Actions of gamma-aminobutyric acid on neurones of guinea-pig myenteric plexus. Br J Pharmacol 1984; 82(1): 93–100.

16 Bertrand PP, Galligan JJ. Alfaxalone, pentobarbital and diazepam potentiate gamma-aminobutyric acid-induced depolarizations in single myenteric neurons of guinea pig intestine. J Pharmacol Exp Ther 1992; 262(2): 677–682.

17 Zhou X, Galligan JJ. $GABA_A$ receptors on calbindin-immunoreactive myenteric neurons of guinea pig intestine. J Auton Nerv Syst 2000; 78(2–3): 122–135.

18 Chen G, Trombley PQ, van den Pol AN. Excitatory actions of GABA in developing rat hypothalamic neurones. J Physiol 1996; 494 (Pt 2): 451–464.

19 De Groat WC, Lalley PM, Saum WR. Depolarization of dorsal root ganglia in the cat by GABA and related amino acids: antagonism by picrotoxin and bicuculline. Brain Res 1972; 44(1): 273–277.

20 Bowery NG, Brown DA. Depolarizing actions of gamma-aminobutyric acid and related compounds on rat superior cervical ganglia *in vitro*. Br J Pharmacol 1974; 50(2): 205–218.

21 Akasu T, Munakata Y, Tsurusaki M, Hasuo H. Role of GABAA and GABAC receptors in the biphasic GABA responses in neurons of the rat major pelvic ganglia. J Neurophysiol 1999; 82(3): 1489–1496.

22 Hills JM, King BF, Mirsky R, Jessen KR. Immunohistochemical localisation and electrophysiological actions of GABA in prevertebral ganglia in guinea-pig. J Auton Nerv Syst 1988; 22(2): 129–140.

23 Sha L, Miller SM, Szurszewski JH. Electrophysiological effects of GABA on cat pancreatic neurons. Am J Physiol Gastrointest Liver Physiol 2001; 280(3): G324–G331.

24 Krantis A, Kerr DI. The effect of GABA antagonism on propulsive activity of the guinea-pig large intestine. Eur J Pharmacol 1981; 76(1): 111–114.

25 Ong J, Kerr DI. $GABA_A$- and $GABA_B$-receptor-mediated modification of intestinal motility. Eur J Pharmacol 1982; 86(1): 9–17.

26 Tonini M, De Petris G, Onori L, Manzo L, Rizzi CA, Crema A. The role of GABAA receptor function in peristaltic activity of the guinea-pig ileum: a comparative study with bicuculline, SR 95531 and picrotoxinin. Br J Pharmacol 1989; 97(2): 556–562.

27 Hardcastle J, Hardcastle PT, Mathias WJ. The influence of the gamma-amino butyric acid (GABA) antagonist bicuculline on transport processes in rat small intestine. J Pharm Pharmacol 1991; 43(2): 128–130.

28 MacNaughton WK, Pineau BC, Krantis A. gamma-Aminobutyric acid stimulates electrolyte transport in the guinea pig ileum *in vitro*. Gastroenterology 1996; 110(2): 498–507.

29 Wouters M, De Laet A, Donck LV, Delpire E, van Bogaert PP, Timmermans JP, de Kerchove d'Exaerde A, Smans K, Vanderwinden JM. Subtractive hybridization unravels a role for the ion cotransporter NKCC1 in the murine intestinal pacemaker. Am J Physiol Gastrointest Liver Physiol 2006; 290(6): G1219–G1227.

30 Sun C, Zhang L, Chen G. An unexpected role of neuroligin-2 in regulating KCC2 and GABA functional switch. Mol Brain 2013; 6: 23.

31 Liu S, Ren W, Qu MH, Bishop GA, Wang GD, Wang XY, Xia Y, Wood JD. Differential actions of urocortins on neurons of the myenteric division of the enteric nervous system in guinea pig distal colon. Br J Pharmacol 2010; 159(1): 222–236.

32 Brookes SJ, Ewart WR, Wingate DL. Intracellular recordings from cells in the myenteric plexus of the rat duodenum. Neuroscience 1988; 24(1): 297–307.

33 Browning KN, Lees GM. Myenteric neurons of the rat descending colon: electrophysiological and correlated morphological properties. Neuroscience 1996; 73(4): 1029–1047.

34 Wood JD. Cellular neurophysiology of enteric neurons. In: Johnson LR, Ghishan FK, Kaunitz JD, Merchant JL, Said HM, Wood JD (eds.). Physiology of the Gastrointestinal Tract. 5th Ed. Academic Press, 2012, 629–669.

35 Hannaert P, Alvarez-Guerra M, Pirot D, Nazaret C, Garay RP. Rat NKCC2/NKCC1 cotransporter selectivity for loop diuretic drugs. Naunyn Schmiedebergs Arch Pharmacol 2002; 365(3): 193–199.

36 Li LS, Liu CZ, Xu JD, Zheng LF, Feng XY, Zhang Y, Zhu JX. Effect of entacapone on colon motility and ion transport in a rat model of Parkinson's disease. World J Gastroenterol 2015; 21(12): 3509–3518.

37 Zhu JX, Yang N, He Q, Tsang LL, Zhao WC, Chung YW, Chan HC. Differential Cl^- and HCO_3^- mediated anion secretion by different colonic cell types in response to tetramethylpyrazine. World J Gastroenterol 2004; 10(12): 1763–1768.

38 Neunlist M, Michel K, Reiche D, Dobreva G, Huber K, Schemann M. Glycine activates myenteric neurones in adult guinea-pigs. J Physiol 2001; 536(Pt 3): 727–739.

39 Pellegrino C, Gubkina O, Schaefer M, Becq H, Ludwig A, Mukhtarov M, Chudotvorova I, Corby S, Salyha Y, Salozhin S, Bregestovski P, Medina I. Knocking down of the KCC2 in rat hippocampal neurons increases intracellular chloride concentration and compromises neuronal survival. J Physiol 2011; 589(Pt 10): 2475–2496.

40 Ben-Ari Y. Excitatory actions of gaba during development: the nature of the nurture. Nat Rev Neurosci 2002; 3(9): 728–739.

41 Starodub AM, Wood JD. Histamine H_2 receptor activated chloride conductance in myenteric neurons from guinea pig small intestine. J Neurophysiol 2000; 83(4): 1809–1816.

42 Kang SH, Vanden Berghe P, Smith TK. Ca^{2+}-activated Cl^- current in cultured myenteric neurons from murine proximal colon. Am J Physiol Cell Physiol 2003; 284(4): C839–C847.

43 Rahmati N, Hoebeek FE, Peter S, De Zeeuw CI. Chloride homeostasis in neurons with special emphasis on the olivocerebellar system: Differential roles for transporters and channels. Front Cell Neurosci 2018; 12: 101.